Gondwe, M.J.; Helfter, C.; Murray-Hudson, M.; Levy, P.E.; Mosimanyana, E.; Makati, A.; Mfundisi, K.B.; Skiba, U.M.. 2021. **Methane flux measurements along a floodplain soil moisture gradient in the Okavango Delta, Botswana [in special issue: Rising methane: is warming feeding warming?** (Part 1)] *Philosophical Transactions of the Royal Society A: Mathematical, Physical and Engineering Sciences*, 379 (2210), 20200448. https://doi.org/10.1098/rsta.2020.0448

Methane flux measurements along a floodplain soil moisture gradient in the Okavango Delta, Botswana

M.J. Gondwe*, C. Helfter†, M. Murray-Hudson*, P.E. Levy†, E. Mosimanyana*, A. Makati*, K.B. Mfundisi*, and U.M. Skiba†.

*Okavango Research Institute, University of Botswana, P/ Bag 285, Maun, Botswana

†UK Centre for Ecology & Hydrology, Bush Estate, Penicuik, Scotland, EH26 0QB, UK

Abstract

Data-poor tropical wetlands constitute an important source of atmospheric CH_4 data-poor in the world. We studied CH_4 fluxes using closed chambers along a soil moisture gradient in a tropical seasonal swamp in the Okavango Delta, Botswana, the 6th largest tropical wetland in the world. The objective of the study was to assess net CH_4 fluxes and controlling environmental factors in the Delta's seasonal floodplains. Net CH_4 emissions from seasonal floodplains in the wetland were estimated at 0.072 ± 0.016 Tg a^{-1}. Microbial CH_4 oxidation of $\sim 2.817 \times 10^{-3} \pm 0.307 \times 10^{-3}$ Tg a^{-1} in adjacent dry soils of the occasional floodplains accounted for the sink of 4% of the total soil CH_4 emissions from seasonal floodplains. The observed microbial CH_4 sink in the Delta's dry soils is therefore comparable to the global average sink of 4-6%. Soil water content (SWC) and soil organic matter (SOM) were the main environmental factors controlling CH_4 fluxes in both the seasonal and occasional floodplains. The optimum SWC for soil CH_4 emissions and oxidation in the Delta were estimated at 50% and 15%, respectively. Electrical conductivity (EC) and pH were poorly correlated ($r^2 \leq 0.11$, $p < 0.05$) with CH_4 fluxes in the seasonal floodplain at Nxaraga.

Key words: seasonal floodplains, methane emissions, methane oxidation, occasional floodplains, tropical wetland.

1. Introduction

Global warming is associated with increasing atmospheric concentrations of greenhouse gases (GHGs) such as nitrous oxide (N_2O), carbon dioxide (CO_2) and methane (CH_4) [1-3]. Methane is currently the second most abundant GHG in the atmosphere after CO_2 [4]). In the period between 1800 and the 1990s atmospheric concentrations of CH_4 increased; then stabilised at approximately 1775 ppb between 1999 and 2006 [5, 6]. Renewed growth in global atmospheric CH_4 concentrations started in 2007 [6-8]. The reasons for the stabilisation and the renewed growth of ~6 Tg CH_4 a^{-1} or ~3% increase in atmospheric CH_4 concentration per year [9,10] since 2007 remain poorly understood due to seemingly contradicting findings, especially pertaining to the magnitudes of CH_4 sources estimated using different methods, by various research works on the issue [6, 9, 10].

According to Dlugokencky et al. [8] and [10], the 2007 renewed growth in atmospheric CH_4 concentration is consistent with abrupt increases in CH_4 emissions from biomass burning and wetlands as well as a reduction in the tropospheric hydroxyl radical (OH) sink of CH_4. Tropical and subtropical wetlands remain the world's largest natural source of CH_4 to the atmosphere [11, 12], accounting for 70% of the global wetland emissions budget [12, 13]. However, estimates of natural CH_4 sources and sinks, particularly in the South American, African and Asian tropics, remain poorly constrained, and with uncertain attribution to the various biogenic and anthropogenic sources [14, 15], thereby hindering development and evaluation of regional and global CH_4 budgets. Methanotrophic CH_4 oxidation, the only known biological sink of atmospheric CH_4, is also poorly understood [16] despite accounting for 4-6% of the total atmospheric CH_4 sink [17].

The aim of this study was to address the uncertainty of CH_4 fluxes, particularly net CH_4 fluxes and controlling environmental factors, from the alluvial Okavango Delta wetlands in Botswana, which is the world's 6th largest wetland. The Okavango Delta consists of permanent

and seasonal wetlands bordering onto dry, occasionally flooded grassland and forest areas (Figure 1a). We report the first chamber-based CH_4 flux measurements along a soil moisture gradient in a seasonal floodplain in the Okavango Delta.

2. Materials and Methods

a) Study site

The Okavango Delta (Figure 1a) is an alluvial wetland with a total area of ~22,000 km^2 and a very low average gradient (1:3600) [18]. The Delta is recharged by flood-pulsed inflow of approximately 10 x 10^9 m^3 a^{-1} (range of 7-15 x 10^9 m^3 a^{-1}; [19, 20]) via the Okavango River which drains the central Angolan highlands located in a subtropical and humid climate with precipitation of up to 1300 mm a^{-1} [21, 22]. An additional water input into the Delta comes from seasonal, erratic and localised convective rainfall over the wetland area averaging 490 mm a^{-1} (equivalent to 6 x 10^9 m^3 a^{-1}) between December and April, peaking in February [20]. Due to the semi-arid conditions in the region, annual evapotranspiration in the Delta exceeds precipitation by a factor of more than 3, such that the system loses 98% of the total water inflow to the atmosphere. The remaining 2% exits the Delta as river outflow through the Boro/Thamalakane and Kunyere Rivers (Figure 1a & b) [19, 23].

The Delta can be divided into three broad ecological zones based on their hydroperiods: the permanent swamp, the seasonal floodplains and the occasional floodplains (Figure 1a). The permanent swamp which covers a maximum area of about 3,000 km^2 consists of the Panhandle and the upper fan area, and is sustained by a base flow of ~150 m^3 s^{-1} of the Okavango River [21]. The permanent swamp is dominated by dense vegetation stands composed of mainly *Cyperus papyrus* and *Phragmites australis* [20]. Most of the flood water in the swamp flows laterally through the dense vegetation [20], which, together with the low gradient, significantly

decrease water velocity through the swamp, and consequently sediment and nutrient transport into the seasonal floodplains [24]).

The flooding of the southern distal areas of the alluvial fan creates seasonal floodplains, which typically last for 6-8 months depending on local summer rainfall and annual volume of inflow via the Okavango River. The seasonal floodplains can cover a total area of more than 3,000 km^2 [25], but flooding extents in excess of 6,000 km^2 have also been reported (see [26]). The flooding is followed by a burst of plant growth dominated by reeds (*Phragmites* spp.) and aquatic herbs (e.g., *Nymphaea* spp., *Potamogeton thunbergii*) in areas subject to longer and deeper floods (e.g., channels and lagoons), and sedges (e.g., *Cyperus articulatus*, *Schoenoplectus corymbosus*) in regularly inundated floodplain areas while grasses (e.g., *Miscanthus junceus*, *Panicum repens*, *Oryza longistaminata* and *Leersia hexandra*) dominate at the floodplain-woodland fringes [27-29]. Dry floodplain fringes are typically dominated by broad-leaved evergreen trees such as *Croton megalobotrys*, *Diospyros mespiliformis*, *Garcinia livingstonei*, and *Ficus sycomorus* [30], while occasionally flooded areas (approx. once in a decade) in more distal locations are usually dominated by grasses such as *Urochloa* sp., *Eragrostis* spp. and *Aristida* spp. [27]. The plant species composition is therefore dependent on zone topography and hydroperiod across the floodplain areas [30, 31]. The seasonal floodplains are heavily utilised for grazing and water by large numbers of wildlife species especially during the dry season when forage and water are scarce in the surrounding upland areas [32].

A substantial amount of water is lost to the atmosphere through evapotranspiration in the seasonal floodplains especially during maximum inundation. The evapotranspirative water loss by plants results in the accumulation of solutes (e.g., calcium, magnesium, potassium, silica and sodium) and nutrients (e.g., nitrogen and phosphorus) in soil water particularly under islands fringed by a variety of broad-leaved, evergreen trees and shrubs (see above). The evapo-

100 transpirative removal of solutes and nutrients from floodplain surface waters maintains the
101 Okavango Delta as a freshwater system despite centuries of solute loading [33, 34]. Most
102 seasonal floodplains in the Okavango Delta experience regular fire activities during the dry
103 winter period between May and September, which consumes most of the above ground dry
104 vegetation and litter [35].

105 The high level of herbivory, low incident rainfall, infertile sandy soils and frequent fire
106 events result in low accumulation of vegetation biomass in these seasonal floodplains
107 compared to the permanent swamps [35]. In addition, the organic matter accumulated during
108 wet periods may experience extensive aerobic decomposition during the dry season [36]. The
109 arenosols consist predominantly of sands (up to 85% [37]) with an increase in peat and other
110 organic material as distance to the river channel decreases thus creating an 'O' horizon in the
111 lower seasonal floodplains. The predominant soils in this region are bright, well- drained sands
112 or loamy sands (Haplic Arenosols) and dark greyish brown, poorly drained sandy loams or
113 clays (Eutric Gleysols) [38].

114 We established a spatial transect to study soil CH_4 emissions using closed chambers in
115 a seasonal floodplain at Nxaraga (Figure 1b) on the southwest side of the Chief's Island in the
116 Okavango Delta, Botswana. The floodplain is bounded to the west by the Boro River, which is
117 one of the main channel systems and outlets of the Delta. The transect was constructed to span
118 dry to waterlogged soils across the floodplain following the moving flood-water edge (Figure
119 2). Site 1 (19°32′52.40″S, 23°10′44.75″E) on rarely flooded dry soils was the only fixed site
120 on the transect because it remained accessible throughout the sampling period (Figure 1b). Site
121 2 slightly fluctuated but was basically located at the edge of the floodplain (where the water
122 front reached) at highstand. Locations of Sites 3 to 7 depended on the length of the remainder
123 of the transect which was equally portioned into additional 2 to 5 sites, partly determined by
124 visual changes (especially wetness) in substrate conditions. The number of measurement sites

125 therefore varied from a maximum of 7 sampling sites at lowstand (during the peak of the dry
126 season) to a minimum of 4 sampling sites at highstand (at maximum flooding extent) (Figure
127 2). A total of 16 field campaigns were conducted over a 2-day period almost monthly from
128 February 2018 to August 2020. Sampling was, however, not done regularly according to plan
129 (monthly) due to unforeseen circumstances, primarily poor accessibility (by boat and vehicle)
130 of the seasonal floodplain from Maun during certain seasons.
131
132 b) Measurements of CH_4 fluxes
133 CH_4 fluxes were measured using a closed dynamic chamber system comprising a
134 transparent cylindrical polycarbonate chamber (388 mm dia., 305 mm high) placed on a pre-
135 installed base, coupled to an ultra-portable GHG Analyzer (GGA, model 915-0011, Los Gatos
136 Research (LGR), Mountain View, CA, USA). The performance of the generally robust GGA
137 was checked at the UK-CEH for compliance with the World Meteorological Organization
138 (WMO) requirements prior to the field campaign in the Okavango Delta, Botswana, using 3-
139 point concentration standards calibrated relative to the WMO CH4-X2004 scale and WMO
140 CO2-X2007 scale for CH_4 and CO_2, respectively. In the field, a set of three plastic chamber
141 bases were installed at each site along the transect at least 12 hours prior to gas measurements,
142 these were removed soon after the measurements to avoid trampling by wildlife. The flow rate
143 through the GGA absorption cell during measurements was 0.5 L min^{-1} and the chamber +
144 tubing volume to surface area ratio was 30.5 cm^3 cm^{-2}. The air in the chamber was continuously
145 mixed during measurements using a compact fan mounted on the lid of the chamber. The
146 chamber operated as a closed system, meaning that the sample air was continuously withdrawn
147 from the chamber headspace, passed through the GGA for simultaneous CO_2, CH_4 and H_2O
148 measurements and returned to the chamber. Each chamber measurement lasted 10 minutes and
149 the GGA reported gas concentrations as dry mole fractions in ppm at 8 seconds intervals. The

150 use of the GGA offers several advantages over laboratory gas chromatographs (GCs)
151 commonly used to measure GHG fluxes. For instance, the sensitivity of infrared spectrometer
152 technology used in the GGA is 500 times better than that of most GCs [39], accurate
153 measurements of multiple gaseous components are taken in real time, the number of
154 measurements obtained for calculating fluxes is many times larger, and a shorter enclosure time
155 can be used. Diurnal variations were very small [40].
156 CH_4 fluxes from the seasonal floodplain were also measured using eddy-covariance
157 equipment also deployed along the study transect (Figure 1b) as a separate but complementary
158 project reported elsewhere [41], except for comparison with the chamber-based fluxes.
159
160 c) Flux calculation
161 For each chamber measurement, the flux of CH_4 was estimated from the time series of
162 CH_4 mixing ratio (nmol mol^{-1}) with time. Because the response often deviates from linear, the
163 initial rate of change dC/dt at t=0 has to be inferred from the data using an appropriate model.
164 Here, we fitted four models to the data (linear, quadratic, asymptotic, and the HMR models
165 [42]) and used the approach of Levy et al. [43] to choose the most appropriate estimate, based
166 on goodness-of-fit criteria. Fluxes were calculated using the R statistical software. For plotting
167 and statistical analysis, Sigmaplot 14.0 software (Systat Software Inc., San Jose, CA, USA)
168 was used.
169
170 d) Soil measurements
171 Soil temperature was measured next to the chamber base at a depth of approximately
172 10 cm using a Hygiplas digital thermometer (model GH628 with accuracy of ±1°C) during
173 each chamber measurement event. After flux measurements were completed, soil samples (0 -
174 10 cm depths) were cored inside each chamber base, using a regular soil auger and stored in

175 airtight double-zipper plastic bags, yielding three sediment/soil cores at each site. These
176 samples were analysed for soil pH, electrical conductivity (EC), soil water content (SWC) and
177 soil organic matter (SOM) content using standard methods at the Environmental Laboratory,
178 Okavango Research Institute, Maun, Botswana. Soil pH was determined potentiometrically
179 according to Hendershot et al. [44] using a pH meter (WTW Inolab pH7110, Weilheim,
180 Germany) after suspension in 1:2.5 (m/v) soil / water ratio. Soil EC was measured two hours
181 later on the same 1:2.5 (m/v) soil / water suspension using a WTW Inolab Cond7110 meter,
182 Weilheim, Germany [45]. SWC and SOM were determined using the gravimetric methods and
183 reported on a dry weight basis. SWC, defined as the ratio of the mass of water present to the
184 dry weight of the soil sample, was determined using homogeneously-mixed wet soil
185 subsamples weighed before and after drying to constant weight at 105 ºC for 24 hours in a
186 Scientific Series 2000 oven (RSA). SOM was estimated by weight loss-on-ignition [46]. A
187 previously oven-dried (at 105 ºC) soil subsample (5.000 ± 0.005 g) was combusted in a
188 Carbolite muffle furnace (UK) at 550 ºC for two hours in pre-weighed clean ceramic porcelain
189 crucibles, cooled to room temperature, and reweighed. SOM (%) was calculated as the
190 difference between the oven-dry soil mass and the soil mass after combustion at 550 ºC, divided
191 by the oven-dry soil mass.
192
193 3. Results
194 The length of the transect which was not inundated (Figure 1b)) ranged from
195 approximately 52 m at maximum flooding (hightand) to 260 m at minimum flooding
196 (lowstand) (Figure 3). Soil temperature across the floodplain transect during the study period
197 was recorded at 24.8 ± 0.8 °C (mean ± SE).
198 Site 1 was characterised by dry soils and patches of salt deposits, common in central
199 areas of most islands in the Okavango Delta, were conspicuous at the soil surface. Because of

this, a much higher soil EC value (mean ± SE) of 578.3 ± 75.7 µS cm^{-1} was recorded at Site 1 compared to a mean of 91.6 ± 8.3 µS cm^{-1} observed at the other measurement sites along the floodplain transect. During 12 of the 16 monthly sampling campaigns, we observed a gradient of decreasing EC values along the transect from Site 1 to the flood water front (Figure 4a). Soil pH showed an exponential decline from dry soils at Site 1 to the river channel (Figure 4b). Soil pH was significantly higher ($p < 0.05$) at Site 1 (9.6 ± 0.1) than the mean pH of 5.7 ± 0.1 at the other sites along the floodplain transect.

SWC and SOM increased with distance along the floodplain transect to the river channel (Figure 5a & b). The mean SWC and SOM recorded at sites 1 and 2 were 13.40 ± 1.13 % SWC and 4.90 ± 0.71% SOM, which increased to 73.28 ± 7.01% SWC and 16.12 ± 1.42% SOM between sites 5 and 7. SWC and SOM values at littoral floodplain sites (sites 1, 2 & 3 at 0, 40 & 70 m average distance along the transect, respectively) tended to be negatively correlated ($r^2 = 0.4646$, $p < 0.05$ at site 3; Figure 6a), but positively correlated ($r^2 = 0.4694$, $p < 0.05$) at the lower floodplain sites 4-7 (Figure 6b). In general, aggregated SWC and SOM data from sites 1-7 were positively correlated ($r^2 = 0.5469$, $p < 0.05$; Figure 6c).

Methane emissions increased from the littoral site (Site 1) to the flood water front during all sampling campaigns (Figure 7a). The mean CH_4 flux rate for all samples collected at sites 2 to 7 during the whole sampling campaign between February 2018 and August 2020 was 44.89 ± 10.80 nmol m^{-2} s^{-1}. In contrast, CH_4 oxidation was primarily recorded at Site 1 (and sporadically at site 2), and the mean flux was - 0.79 ± 0.09 nmol m^{-2} s^{-1}.

Soil pH and EC were poorly correlated ($r^2 \leq 0.11$) with CH_4 fluxes (Figure 7b & c). However, emissions were generally higher (>100 nmol CH_4 m^{-2} s^{-1}) between pH 5.0 and pH 6.6 and EC of less than 200 µS cm^{-1}. CH_4 emissions showed a tendency to increase as SOM (Figure 8a) and SWC (Figure 9a) increased along the study transect. Similarly CH_4 oxidation

224 increased, especially at Site 1, as SOM and SWC increased from 2-5% (Figure 8b) and 3-15%
225 (Figure 9b), respectively. Higher SOM and SWC favored CH_4 emission rather than oxidation.
226 Soil CH_4 fluxes measured by the closed chamber technique agreed reasonably well with
227 their eddy-covariance counterparts in 2018 and 2019 (Figure 10). To facilitate the comparison
228 between the two techniques, eddy-covariance data were selected for monthly averaging if the
229 flux footprint was consistent with the portion of the floodplain where chamber measurements
230 took place. Without that condition on the extent of the flux footprint, the eddy-covariance
231 fluxes were an order of magnitude larger than the chambers values in 2019, but still comparable
232 in 2018.
233
234 4. Discussion
235 The data reported here spans the period from February 2018 to August 2020. During
236 this period, the Okavango Delta experienced a significant reduction in water inflow via the
237 Okavango River. For instance, the maximum inundation extent in the Delta estimated from
238 MODIS imagery [47] declined from > 11000 km^2 in 2010-2012 to < 3500 km^2 in 2019
239 (http://www.okavangodata.ub.bw/ori/monitoring/flood_maps/). Consequently most seasonal
240 floodplains, including Nxaraga floodplain, received little or no flooding especially during the
241 2019 flood season. The drought is likely to have affected biogeochemical processes in the
242 floodplain soils including decomposition of organic matter, CH_4 production and oxidation, and
243 net fluxes [48, 49].
244 The role of pH on methanogenic and methanotrophic microbial activities is dynamic.
245 For example, Valentine et al. [50] found a correlation between pH and potential CH_4 production
246 in laboratory experiments, whilst Moore and Knowles [51] found no relationship. At the global
247 scale, Wen et al. [52] reported that temperature and soil pH are major controllers of
248 methanogenesis. At Nxaraga seasonal floodplain, pH across the transect varied widely and

ranged from pH 4.2 to pH 10.5. The pH decreased from dry soils at Site 1 to the edge of the Boro channel, as previously reported by Bonyongo et al. [53]. The variability was much larger across the lower floodplain area (pH 4.2-9.1 between Sites 2-7) than at the dry soil Site 1 (pH 8.6-10.5). According to Segers [54], the optimum pH for most methanogenic bacteria is 7.0. However, only 8% of the 112 soil pH measurements along the transect at Nxaraga were between pH 6.7 and 7.3. Approximately 73% of the pH measurements were lower than 6.7, which could mean that methanogens in the floodplain soils have adapted to the slightly acidic conditions such that the highest CH_4 emissions were recorded at soil pH between 5.0-6.6 (Figure 7a) [55]. Much higher soil pH values (8.6-10.5) at Site 1, were probably influenced by the salt deposits at the site (see EC below) and was the only site where CH_4 was oxidised almost consistently throughout the study period, with an average flux of - 0.79 ± 0.09 nmol m^{-2} s^{-1}. Most methanotrophs operate around neutral pH, except for some species, which have adapted to high alkalinity situations, such as a highly alkaline soda lake (pH 9.5) in Central Asia [56]. Since salt deposits are common in forested island soils in the Okavango Delta, the methanotrophs are likely to have adapted to the high alkalinity in these soil environments.

Water EC, a measure of salinity, generally increases due to evapo-concentration as the flood water traverses the Okavango Delta to distal areas. A significant amount of water in floodplains around forested islands experiences a strong radial flow to the centre of islands induced by evapotranspiration of broad-leaved evergreen trees on the fringes of the islands. The process consequently concentrates solutes in the island fringe soils and in soil water underneath the islands. This permanent burial of solute beneath islands is the main process that maintains the Okavango Delta as a freshwater ecosystem [33, 34]. As the floodwaters recede, some of the remaining solutes are deposited on the rest of the floodplain soils causing an island-floodplain EC gradient (Figure 4a). While salinity, defined as EC > 4000 µS cm^{-1}, depresses both methanogenic and methanotrophic activities [57], the much lower EC values (this study)

measured at Nxaraga floodplain sites did not seem to affect CH_4 fluxes. Most of the higher fluxes (>100 nmol CH_4 m^{-2} s^{-1}) were observed at soil EC < 200 µS cm^{-1}, whilst high EC values, measured at the dry soil site, were accompanied by net microbial CH_4 oxidation.

The importance of SWC and SOM in controlling CH_4 emission and oxidation processes has been presented in literature [58]. CH_4 emission is a net result of its production by methanogens and consumption by methanotrophs in anaerobic and aerobic soils, respectively [55, 59]. Figures 7 and 8 show clear effects of SOM and SWC on both CH_4 emission and oxidation in the seasonal floodplain at Nxaraga.

Although the range of soil CH_4 fluxes along the study transect was large, the fluxes increased with SOM in the seasonal floodplain (Figure 8a). A significant positive correlation ($r^2 = 0.1465$, $p < 0.05$) was observed between natural-log transformed soil CH_4 flux and SOM data (figure not shown). The high CH_4 fluxes increased rapidly to a threshold of about 300-400 nmol m^{-2} s^{-1} at SOM contents of approximately 7-8% (Figure 8a). Soil CH_4 emissions and SOM correlate mainly because the SOM provides substrates for methanogenic CH_4 production whilst its decomposition maintains anaerobic soil conditions by consuming dissolved O_2 and other available alternative electron acceptors such as NO_3^-, Fe^{3+}, Mn^{4+} and SO_4^{2-} [60]. Soil CH_4 emissions were found to be strongly correlated to SWC between the ranges 15-150% (Figure 9a). An optimum SWC for CH_4 emission has been therefore estimated at 50%, beyond which SWC appears to suppress soil CH_4 emission by constraining the diffusivity of CH_4 to the atmosphere (Figure 9a). However, more sampling is needed to confirm the optimum SWC required for soil CH_4 emissions by sampling multiple seasonal floodplains because it is an important environmental factor for modelling CH_4 emissions in the Okavango Delta and potentially further afield.

Once emitted, the CH_4 may remain in the atmosphere where it acts as a potent GHG with a global warming potential 28 times that of CO_2, or it may diffuse into the dry soil matrix

299 with subsequent oxidation to CO_2 by methanotrophic bacteria. The widespread aerobic
300 microbial CH_4 oxidation which occurs primarily within the top 10 cm layer of undisturbed soils
301 [61-63], is the only known biological sink of this GHG and accounts for 4-6% of the total
302 global CH_4 sink strength [17]. Soil CH_4 oxidation therefore has a direct effect on net CH_4
303 emissions from the environment. The rate of soil CH_4 oxidation depends on the microbial
304 activity of methanotrophs and the rate of diffusion of atmospheric CH_4 within the soil profile
305 [64, 65]. The microbial CH_4 oxidation process, just like CH_4 production by methanogens, is
306 regulated by a number of environmental factors such as SWC, SOM, temperature, pH and soil
307 nitrogen content [59, 66]. The rate of diffusion of atmospheric CH_4 and O_2 into the soil matrix
308 for CH_4 oxidation is controlled primarily by SWC and the physical soil structure (e.g., soil
309 texture and compaction) such that water-logged and fine-textured soils, for instance, have low
310 gas diffusivity [59, 65]. In fact, gas transport into the soil matrix has been suggested to be the
311 main rate limiting factor for atmospheric CH_4 oxidation in soils [67]. In the current study,
312 although SWC and SOM at Site 1 varied within a narrow range, soil CH_4 oxidation at the site
313 increased with both SOM (Figure 8b) and SWC (Figure 9b). The optimum SWC for CH_4
314 oxidation (where more negative fluxes were observed) in dry soils at Nxaraga was estimated
315 at approximately 15% (Figure 9b): lower and higher SWC values seem to supress CH_4
316 oxidation, either by physiological water stress of methanotrophs at very low SWC or by
317 restricting supply of both CH_4 and O_2 required for aerobic soil methanotrophic activity at
318 higher SWC [58, 65]. The optimum SWC of 15% for soil CH_4 oxidation observed at Nxaraga
319 is consistent with optimum SWCs for methanotrophic activities reported in previous studies:
320 11% SWC in Whalen et al. [68] and 20% SWC in Castro et al. [69]. The variation has been
321 suggested to primarily depend on soil type [70]. Figure 9a further suggests that SWC values
322 between 15 and 50% enhance CH_4 emission, rather than oxidation, from the seasonal floodplain
323 soils because as SWC increases, it simultaneously creates conducive anaerobic conditions for

CH_4 production when substrates are available and lowers its oxidation rate by restricting O_2 supply into the soil [55, 59]. It was not possible to estimate the optimum SOM for soil CH_4 oxidation from the data currently available for the Delta, and therefore calls for more research on the effect of SOM and other environmental factors, including soil inorganic nitrogen concentration, not assessed in this study.

5. Upscaling of CH_4 emission and oxidation rates to the whole Okavango Delta

The mean CH_4 emission rate measured by closed chambers at Nxaraga (44.89 ± 10.80 nmol m^{-2} s^{-1}, equivalent to 2.61 ± 0.62 mg CH_4 m^{-2} h^{-1}) is comparable with emissions from several tropical wetlands across the world (range 0.003-40.4 mg CH_4 m^{-2} h^{-1} and mean of 7.67 mg CH_4 m^{-2} h^{-1}), including the Congo River Basin with a CH_4 flux of 4.41 mg m^{-2} h^{-1} [71]. The mean CH_4 flux rate at Nxaraga is also comparable to fluxes from 71 northern, temperate and subtropical wetlands where mean fluxes were reported at 2.01 ± 0.16 mg CH_4 m^{-2} h^{-1} for subtropical, 3.03 ± 0.05 mg CH_4 m^{-2} h^{-1} for boreal, 4.54 ± 0.19 mg CH_4 m^{-2} h^{-1} for temperate and 4.68 ± 0.26 mg CH_4 m^{-2} h^{-1} for subarctic wetlands [72]. A more recent analysis of global natural wetlands estimated CH_4 emissions at 2.01 mg CH_4 m^{-2} h^{-1} (range 1.37 – 2.43) [15]. Similarly, the soil CH_4 oxidation rates (0.046 ± 0.005 mg m^{-2} h^{-1} observed at Nxaraga are also comparable to mean CH_4 oxidation rates of 0.13 to 2.02 mg m^{-2} h^{-1} recorded in northern, temperate and subtropical wetlands [72].

Although uncertainties of these flux estimates are large, the similarity in CH_4 flux rates observed in different wetlands and parts of the world is noteworthy. Research on CH_4 fluxes from wetlands is generally skewed towards arctic and temperate climate wetlands, with fewer studies from tropical and subtropical climate zones. This imbalance needs to be addressed in order to better model the global CH_4 budget.

348 Chamber fluxes are representative of small scale biophysical and biogeochemical
349 processes and spatial heterogeneity can make upscaling to plot or landscape scales challenging
350 although strong agreements between upscaled chamber fluxes and fluxes derived by other
351 techniques such as eddy-covariance have been reported [73-76]. In this study, a good
352 agreement (r^2 = 0.8102, p = 0.0002) was also observed using monthly averaged areal CH_4
353 fluxes in 2018 and 2019 from the chamber and eddy-covariance techniques (Figure 10).
354 Gumbricht et al. [25] estimated the total area of the Okavango wetland at 13693 km^2,
355 about 22%, 24% and 54% of which are permanently, seasonally and occasionally flooded areas
356 of the system. These figures have been recently revisited to take into account the climatic and
357 developmental changes the Okavango basin, which includes the Delta, has experienced over
358 the past two decades. While seasonal floodplains are inundated almost annually, occasional
359 floodplains are flooded only during high floods, which occur approximately once in a decade,
360 and can therefore be considered as dry areas capable of CH_4 oxidation as observed at inland
361 Site 1 in this study. Assuming that Site 1 at Nxaraga (where CH_4 oxidation > CH_4 production)
362 is a proxy for the occasionally flooded wetlands and that sites 2-7 (where CH_4 production >
363 CH_4 oxidation) are representative of seasonal floodplains in the Okavango Delta, we estimate
364 the net CH_4 emission for these two hydrological zones to be of the order of 0.072 ± 0.016 Tg
365 a^{-1} with net emissions at seasonal swamps of 0.075 ± 0.018 Tg a^{-1} and net oxidation in
366 occasional swamps of the order of $2.817 \times 10^{-3} \pm 0.307 \times 10^{-3}$ Tg a^{-1}. These estimates suggest
367 that the biological CH_4 sink in the occasional floodplain soils in the Delta is small as it accounts
368 for only 4% of the total CH_4 emissions in the seasonal floodplains in the wetland. The fraction
369 of the atmospheric CH_4 associated with the biological sink in the Okavango Delta is, however,
370 comparable to the global average sink of 4-6% [17]. There is however need for more research
371 in soil CH_4 oxidation in the Delta since the current study sampled only one site that may not
372 adequately represent the vast areas of the occasionally flooded wetlands of the system.

6. Conclusion

This study estimated chamber-based CH_4 emission and oxidation rates in a seasonal floodplain in the Okavango Delta at 44.89 ± 10.80 nmol m^{-2} s^{-1} and 0.79 ± 0.09 nmol m^{-2} s^{-1}, respectively. Although measurements were done during a relatively dry period for the Delta, the observed CH_4 fluxes are comparable to fluxes in other wetlands across the world. The observed CH_4 oxidation which was upscaled to the whole dry occasionally flooded swamp area of the Okavango Delta accounted for approximately 4% of the total CH_4 emissions from the Delta's seasonal floodplains. The Delta's CH_4 sink due to methanotrophic activity is also comparable to the global average biological sink of 4-6%. As in other wetlands, SWC followed by SOM were found to be the main environmental factors controlling CH_4 fluxes in seasonal swamps in the Delta. Maximum CH_4 emission and oxidation rates in the seasonal floodplain at Nxaraga were observed at 50% and 15% SWC. Electrical conductivity (EC) and pH were not correlated with CH_4 fluxes in the seasonal floodplains. Upscaling of CH_4 oxidation fluxes were achieved from measurements at only one dry soil site. Future studies should, therefore, attempt to measure CH_4 oxidation fluxes at several dry soil sites in different drylands (e.g., grasslands, woodlands, forests) of the Okavango Delta.

Acknowledgements

This work was funded by the UK Natural Environment Research Council (NERC) through the Global Methane Budget project (grant numbers NE/N015746/1 and NE/N015746/2). We thank the UK Centre for Ecology & Hydrology (UKCEH) for availing research equipment. We also thank the Okavango Research Institute and its Environmental Laboratory for additional research equipment, field logistics and sample analysis.

398 References

399 1. IPCC 1996 Climate change 1995: the science of climate change: contribution of working
400 group I to the second assessment report of the intergovernmental panel on climate change.
401 In: Houghton JT, Meira Filho LG, Callander BA, Harris N, Kattenberg A, Maskell K (eds).
402 Cambridge, UK, Cambridge University Press. p 572
403 2. Wang Z, Zeng D, Patrick WH. 1996 Methane emissions from natural wetlands. *Environ*
404 *Monit. Assess*. 42: 143-161. (doi.org/10.1007/BF00394047)
405 3. Johansson AE, Gustavsson A-M, Oquist MG, Svensson BH. 2004 Methane emissions from
406 a constructed wetland treating wastewater - seasonal and spatial distribution and
407 dependence on edaphic factors. *Water Res.* 38: 3960-3970.
408 (doi.org/10.1016/j.watres.2004.07.008)
409 4. Nahlik AM, Mitsch WJ. 2011 Methane emissions from tropical freshwater wetlands
410 located in different climatic zones of Costa Rica. *Glob Change Biol*. 17: 1321-1334.
411 (doi.org/10.1111/j.1365-2486.2010.02190.x)
412 5. Dlugokencky EJ, Houweling S, Bruhwiler L, Masarie KA, Lang PM, Miller JB, Tans PP.
413 2003 Atmospheric methane levels off: Temporary pause or a new steady-state? *Geophys.*
414 *Res. Lett.* 30(19): 1992. (doi:10.1029/2003GL018126)
415 6. Turner AJ, Frankenberg C, Wennberg PO, Jacob DJ. 2017 Ambiguity in the causes for
416 decadal trends in atmospheric methane and hydroxyl. *PNAS* 114(21): 5367-5372.
417 (doi.org/10.1073/pnas.1616020114)
418 7. Rigby M *et al*. 2008 Renewed growth of atmospheric methane. *Geophys Res. Lett.* 35:
419 L22805. (doi:10.1029/2008GL036037)
420 8. Dlugokencky EJ *et al*. 2009 Observational constraints on recent increases in the
421 atmospheric CH_4 burden. *Geophys. Res. Lett.* 36: L18803.
422 (doi.org/10.1029/2009GL039780)

9. Kirschke S *et al.* 2013 Three decades of global methane sources and sinks. *Nat. Geosci.* 6: 813-823. (doi.org/10.1038/ngeo1955)
10. Nisbet EG, Dlugokencky EJ, Bousquet P. 2014 Methane on the rise again. *Science* 343(6170): 493-495. (doi: 10.1126/science.1247828)
11. Bousquet P *et al*. 2011 Source attribution of the changes in atmospheric methane for 2006–2008. *Atmos. Chem. Phys.* 11: 3689–3700. (doi: 10.5194/acpc-10-27603-2010)
12. Bloom AA, Palmer PI, Fraser A, Reay DS, Frankenberg C. 2010 Large-scale controls of methanogenesis inferred from methane and gravity spaceborne data. *Science* 327 (5963): 322-325. (doi: 10.1126/science.1175176)
13. Meng, L., R. Paudel, P.G.M. Hess and N.M. Mahowald. 2015. Seasonal and interannual variability in wetland methane emissions simulated by CLM4Me' and CAM-chem and comparisons to observations of concentrations. *Biogeosciences* 12: 4029–4049. (https://doi.org/10.5194/bg-12-4029-2015)
14. Saunois M *et al*. 2016 The global methane budget 2000 - 2012. *Earth Sys. Sci. Data* 8: 697-751. (doi.org/10.5194/essd-8-697-2016)
15. Saunois M *et al*. 2020 The Global Methane Budget 2000–2017. *Earth Sys. Sci. Data* 12: 1561-1623. (doi.org/10.5194/essd-12-1561-2020)
16. Valenzuela EI *et al*. 2017 Anaerobic methane oxidation driven by microbial reduction of natural organic matter in a tropical wetland. *Appl. Environ. Microbiol.* 83: e00645-17. (doi.org/10.1128/AEM.00645-17)
17. Ciais P *et al*. 2013 Carbon and other biogeochemical cycles. In *Climate Change 2013: the Physical Science Basis. Contribution of Working Group I to the Fifth Assessment Report of the Intergovernmental Panel on Climate Change* (eds TF Stocker *et al*.), pp. 465–570. Cambridge, UK, Cambridge University Press.

18. McCarthy TS, Ellery WN, Ellery K. 1993 Vegatation-induced, subsurface precipitation of carbonate as an aggradational process in the permanent swamps of the Okavango Delta fan, Botswana. *Chem. Geol.* 107: 111-131. (doi.org/10.1016/0009-2541(93)90105-R)
19. SMEC 1987. Southern Okavango Integrated Water Development, Phase 1: Final Report Technical Study. Vol III: Water Resource and Development. Department of Water Affairs, Gaborone, Botswana.
20. McCarthy TS, Ellery WN. 1998 The Okavango Delta. *Trans. R. Soc. S. Afr.* 53(2): 157-182. (doi.org/10.1080/00359199809520384)
21. Milzow C, Tshekiso O, Kgotlhang L, Kinzelbach W. 2010 Sediment transport monitoring and short term modeling in the Okavango Delta, Botswana. *Wetlands* 30: 417-428. (doi: 10.1007/s13157-010-0042-x)
22. King J, Chonguica E. 2016 Integrated management of the Cubango-Okavango River Basin. *Ecohydrol. Hydrobiol.* 16: 263-271. (doi.org/10.1016/j.ecohyd.2016.09.005)
23. Dincer T, Hutton LG, Kupee BBJ. 1981 Study, using stable isotopes, of flow distribution, surface--groundwater relations and evapotranspiration in the Okavango swamp, Botswana. Int. Atomic Energy Agency, Vienna, Proc. Ser. SII/AUB/493, pp. 3-26.
24. McCarthy TS, Ellery WN, Stanistreet IG. 1992 Avulsion mechanisms on the Okavango fan, Botswana: the control of a fluvial system by vegetation. *Sedimentology* 39: 119-195. (doi.org/10.1111/j.1365-3091.1992.tb02153.x)
25. Gumbricht T, McCarthy J, McCarthy TS. 2004 Channels, wetlands and islands in the Okavango Delta, Botswana, and their relation to hydrological and sedimentological processes. *Earth Surf. Proc. Land.* 29:15–29. (doi.org/10.1002/esp.1008)
26. Mladenov N, McKnight DM, Wolski P, Murray-Hudson M. 2007 Simulation of DOM fluxes in a seasonal floodplain of the Okavango delta, Botswana. *Ecol. Model.* 205: 181-195. (doi.org/10.1016/j.ecolmodel.2007.02.015)

27. Bonyongo MC, Bredenkamp GJ, Veenendaal E. 2000 Floodplain vegetation in the Nxaraga Lagoon area, Okavango Delta, Botswana. *S. Afr. J. Bot.* 66(1): 15-21. (doi.org/10.1016/S0254-6299(15)31046-2)
28. Ellery K, Ellery WN, Rogers KH, Walker BH. 1991 Water depth and biotic insulation: major determinants of back-swamp plant community composition. *Wetl. Ecol. Manage.* 1: 149-62. (doi.org/10.1007/BF00177289)
29. Heinl M, Neuenschwander A, Sliva J, Vanderpost C. 2006 Interactions between fire and flooding in a southern African floodplain system (Okavango Delta, Botswana). *Landsc. Ecol.* 21: 699-709. (doi.org/10.1007/s10980-005-5243-y)
30. Ramberg L, Wolski P, Krah M. 2006 Water balance and infiltration in a seasonal floodplain in the Okavango Delta, Botswana. *Wetlands* 26(3): 677–690. (doi.org/10.1672/0277-5212(2006)26[677:WBAIIA]2.0.CO;2)
31. Heinl M, Sliva J, Tacheba B, Murray-Hudson M. 2008 The relevance of fire frequency for the floodplain vegetation of the Okavango Delta, Botswana. *Afr. J. Ecol.* 46(3): 350-358. (doi.org/10.1111/j.1365-2028.2007.00847.x)
32. SMEC 1989. Ecological zoning Okavango Delta. Final Report Volume 1 - Main Report. Kalahari Conservation Society, Gaborone, Botswana.
33. Bauer P, Supper R, Zimmermann S, Kinzelbach W. 2006 Geoelectrical imaging of groundwater salinization in the Okavango Delta, Botswana. *J. Appl. Geophys.* 60: 126-141
34. Ramberg L, Wolski P. 2008 Growing islands and sinking solutes: processes maintaining the endorheic Okavango Delta as a freshwater system. *Plant Ecol.* 196: 215-231. (doi.org/10.1007/s11258-007-9346-1)
35. Heinl M, Frost P, Vanderpost C, Sliva J. 2007 Fire activity on drylands and floodplains in the southern Okavango Delta, Botswana. *J. Arid Environ.* 68: 77-87. (doi.org/10.1016/j.jaridenv.2005.10.023)

497 36. Riley, W.J., Z.M. Subin, D.M. Lawrence, S.C. Swenson, M.S. Torn, L. Meng, N.M.
498 Mahowald and P. Hess. 2011. Barriers to predicting changes in global terrestrial methane
499 fluxes: analyses using CLM4Me, a methane biogeochemistry model integrated in CESM.
500 *Biogeosciences* 8: 1925-1953 (doi.org/10.5194/bg-8-1925-2011)
501 37. Staring GJ. 1978 Soils of the Okavango Delta, Field Document No. 14: Swamp and dryland
502 soils of the Okavango. Project BOT 72/019, UNDP/FAO and Government of Botswana
503 (report and maps).
504 38. De Wit PV, Nachtergaele FO. 1990 Explanatory note on the soil map of the Republic of
505 Botswana. Soil Mapping and Advisory Services, Gaborone.
506 39. Hensen A, Skiba U, Famulari D. 2013 Low cost and state of the art methods to measure
507 nitrous oxide emissions. *Environ. Res. Lett.* 8: 025022. (doi: 10.1088/1748-
508 9326/8/2/025022)
509 40. Gondwe MJ, Masamba WR. 2014 Spatial and temporal dynamics of diffusive methane
510 emissions in the Okavango Delta, northern Botswana, Africa. *Wetlands Ecol. Manage.*
511 22: 63-78. (doi.org/10.1007/s11273-013-9323-5)
512 41. Helfter C, Gondwe MJ, Murray-Hudson M, Makati A, Lunt MF, Palmer PI, Skiba U. 2021
513 Phenology of emergent macrophytes is the dominant control of methane emissions in a
514 tropical non-forested wetland. Submission to Nature Communications.
515 42. Pedersen AR, Petersen SO, Schelde K. 2010 A comprehensive approach to soil-atmosphere
516 trace-gas flux estimation with static chambers. *Eur. J. Soil Sci.* 61: 888-902.
517 (doi.org/10.1111/j.1365-2389.2010.01291.x)
518 43. Levy PE *et al*. 2012 Methane emissions from soils: synthesis and analysis of a large UK
519 data set. *Glob. Change Biol.* 18(5): 1657-1669. (doi.org/10.1111/j.1365-
520 2486.2011.02616.x)

44. Hendershot WH, Lalande H, Duquette M. 2007 Soil reaction and exchangeable acidity. In *Soil sampling and methods of analysis*, 2nd edn (eds MR Carter, EG Gregorich), pp 173-178. Florida, USA, CRC Press.
45. Miller JJ, Curtin D. 2007 Electrical conductivity and soluble ions. In *Soil sampling and methods of analysis*, 2nd edn (eds MR Carter, EG Gregorich), pp 161-171. Florida, USA, CRC Press.
46. Schulte EE, Hopkins BG. 1996 Estimation of organic matter by weight loss-on-ignition. In *Soil organic matter: Analysis and interpretation* (eds FR Magdoff *et al*.), pp. 21-31. Madison, Wisconsin (USA), SSSA. (doi.org/10.2136/sssaspecpub46.c3)
47. Wolski P, Murray-Hudson M, Thito K, Cassidy L. 2017 Keeping it simple: Monitoring flood extent in large data-poor wetlands using MODIS SWIR data. *Int. J. Appl. Earth Obs. Geoinf.* 57**:** 224-234. (doi.org/10.1016/j.jag.2017.01.005)
48. Chamberlain SD, Hemes KS, Eichelmann E, Szutu DJ, Verfaillie JG, Baldocchi DD. 2020 Effect of drought-induced salinization on wetland methane emissions, gross ecosystem productivity, and their interactions. *Ecosystems* 23: 675-688. (doi.org/10.1007/s10021-019-00430-5)
49. Moore BD, Kaur G, Motavalli PP, Zurweller BA, Svoma BM. 2017. Soil greenhouse gas emissions from agroforestry and other land uses under different moisture regimes in lower Missouri River floodplain soils: a laboratory approach. *Agrofor. Syst.* 92(2): 335–348. (doi.org/10.1007/s10457-017-0083-8)
50. Valentine DW, Holland EA, Schimel DS. 1994 Ecosystem and physiological controls over methane production in northern wetlands. *J. Geophys. Res.* 99: 1563-1571. (doi.org/10.1029/93JD00391)
51. Moore TR, Knowles R. 1990 Methane emissions from fen, bog and swamp peatlands in Quebec. *Biogeochemistry* 11: 45-61. (doi.org/10.1007/BF00000851)

546 52. Wen X, Yang S, Horn F, Winkel M, Wagner D, Liebner S. 2017 Analysis of
547 methanogenic archaea identifies community-shaping environmental factors of natural
548 environments. *Front. Microbiol.* 8: 1339. (doi: 10.3389/fmicb.2017.01339)
549 53. Bonyongo MC, Mubyana T, Totolo O, Veenandaal EM. 2002 Flooding and soil nutrient
550 status in the Okavango Delta's seasonal floodplains. *Botsw. Notes Rec.* 34: 123-130.
551 54. Segers R. 1998 Methane production and methane consumption: a review of processes
552 underlying wetland methane fluxes. *Biogeochemistry* 41**:** 23-51.
553 (doi.org/10.1023/A:1005929032764)
554 55. Le Mer J, Roger P. 2001 Production, oxidation, emission and consumption of methane by
555 soils: a review. *Eur. J. Soil Biol.* 37: 25-50. (doi.org/10.1016/S1164-5563(01)01067-6)
556 56. Khmelenina VN, Kalyuzhnaya MG, Starostina NG, Suzina NE, Trotsenko YA.
557 1997 Isolation and characterization of halotolerant alkaliphilic methanotrophic bacteria
558 from Tuva soda lakes. *Curr. Microbiol.* 35: 257-261. (doi.org/10.1007/s002849900249)
559 57. van der Gon HACD, Neue H-U. 1995 Methane emission from a wetland rice field as
560 affected by salinity. *Plant Soil* 170(2): 307-313. (doi.org/10.1007/BF00010483)
561 58. van den Pol-van Dasselaar A, van Beusichem ML, Oenema O. 1998 Effects of soil moisture
562 content and temperature on methane uptake by grasslands on sandy soils. *Plant Soil* 204**:**
563 213–222. (doi.org/10.1023/A:1004371309361)
564 59. Chowdhury TR, Dick RP. 2013 Ecology of aerobic methanotrophs in controlling methane
565 fluxes from wetlands. *Appl. Soil Ecol.* 65: 8-22. (doi:1016/j.apsoil.2012.12.014)
566 60. Heintze G, Eickenscheidt T, Schmidhalter U, Drösler M. 2017 Influence of soil organic
567 carbon on greenhouse gas emission potential after application of biogas residues or cattle
568 slurry: Results from a pot experiment. *Pedosphere* 27(5): 807-821.
569 (doi.org/10.1016/S1002-0160(17)60388-6)

570 61. Adamsen APS, King GM. 1993 Methane consumption in temperate and subarctic forest
571 soils: Rates, vertical zonation, and responses to water and nitrogen. *Appl. Environ.*
572 *Microbiol.* 59: 485-490 (doi: 10.1128/AEM.59.2.485-490.1993)
573 62. Koschorreck M, Conrad R. 1993 Oxidation of atmospheric methanein soil: Measurements
574 in the field, in soil cores and in soil sample. *Global Biogeochem. Cy.* 7: 109-121.
575 (doi.org/10.1029/92GB02814)
576 63. Kruse CW, Moldnip P, Iversen N. 1996 Modelling diffusion and reaction in soils, II,
577 Atmospheric methane diffusion and consumption in soils. *Soil Sci.*. 161: 355-365.
578 (doi.org/10.1097/00010694-199606000-00002)
579 64. Dörr H, Katruff L, Levin I. 1993 Soil texture parameterization of the methane uptake in
580 aerated soils. *Chemosphere* 26: 697–713. (doi.org/10.1016/0045-6535(93)90454-D)
581 65. Lang R, Goldberg SD, Blagodatsky S, Piepho H-P, Hoyt AM, Harrison RD, Xu J, Cadisch
582 G. 2020 Mechanism of methane uptake in profiles of tropical soils converted from forest
583 to rubber plantations. *Soil Biol. Biochem.* 145: 107796.
584 (doi.org/10.1016/j.soilbio.2020.107796)
585 66. Oertel C, Matschullat J, Zurba K, Zimmermann F, Erasmi S. 2016 Greenhouse gas
586 emissions from soils - A review *Chem. Erde* 76: 327-352. (doi.org/10.1016/j.chemer.
587 2016.04.002)
588 67. Topp E, Pattey E. 1997 Soils as sources and sinks for atmospheric methane. *Can. J. Soil*
589 *Sci.* 77: 167-178. (doi.org/10.4141/S96-107)
590 68. Whalen SC, Reeburgh WS, Sandbeck KA. 1990 Rapid methane oxidation in a landfill
591 cover soil. *Appl. Environ. Microbiol.* 56: 3405-3411 (doi: 10.1128/aem.56.11.3405-
592 3411.1990)

69. Castro MS, Steudler PA, Melillo JM. 1995 Factors controlling atmospheric methane consumption by temperate forest soils. *Glob. Biogeochem. Cycles* 9: 1-10. (https://doi.org/10.1029/94GB02651)

70. Schnell S, King GM. 1996 Responses of methanotrophic activity in soils and cultures to water stress. *Appl. Environ. Microbiol.* 62(9): 3203-3209. (doi: 10.1128/aem.62.9.3203-3209.1996)

71. Sjögersten S, Black R, Evers S, Hoyos-Santillan J, Wright EL, Turner BL. 2014 Tropical wetlands: A missing link in the global carbon cycle? *Global Biogeochem. Cy.* 28: 1371-1386. (doi:10.1002/2014GB004844)

72. Turetsky M.R. et al. 2014. A synthesis of methane emissions from 71 northern, temperate, and subtropical wetlands. *Glob. Change Biol.* 20: 2183–2197. (doi: 10.1111/gcb.12580)

73. Riutta T *et al*. 2007. Spatial variation in plant community functions regulates carbon gas dynamics in boreal fen ecosystem. *Tellus* 59B: 838-852. (doi.org/10.1111/j.1600-0889.2007.00302.x)

74. Sachs T, Giebels M, Boike J, Kutzbach L. 2010 Environmental controls of CH_4 emission from polygonal tundra on the micro-site scale, Lena River Delta, Siberia. *Glob. Change Biol.* 16: 3096-3110. (doi.org/10.1111/j.1365-2486.2010.02232.x)

75. Schrier-Uijl AP, Kroon PS, Hensen A, Leffelaar PA, Berendse F, Veenendaal EM. 2010 Comparison of chamber and eddy covariance-based CO_2 and CH_4 emission estimates in a heterogeneous grass ecosystem on peat. *Agric. For. Meteorol.* 150: 825-831. (doi.org/10.1016/j.agrformet.2009.11.007)

76. Levy P, Drewer J, Jammet M, Leeson S, Friborg T, Skiba U, van Oije M. 2020 Inference of spatial heterogeneity in surface fluxes from eddy covariance data: A case study from a subarctic mire ecosystem. *Agric. For. Meteorol.* 280: 107783. (doi.org/10.1016/j.agrformet.2019.107783)

618

619

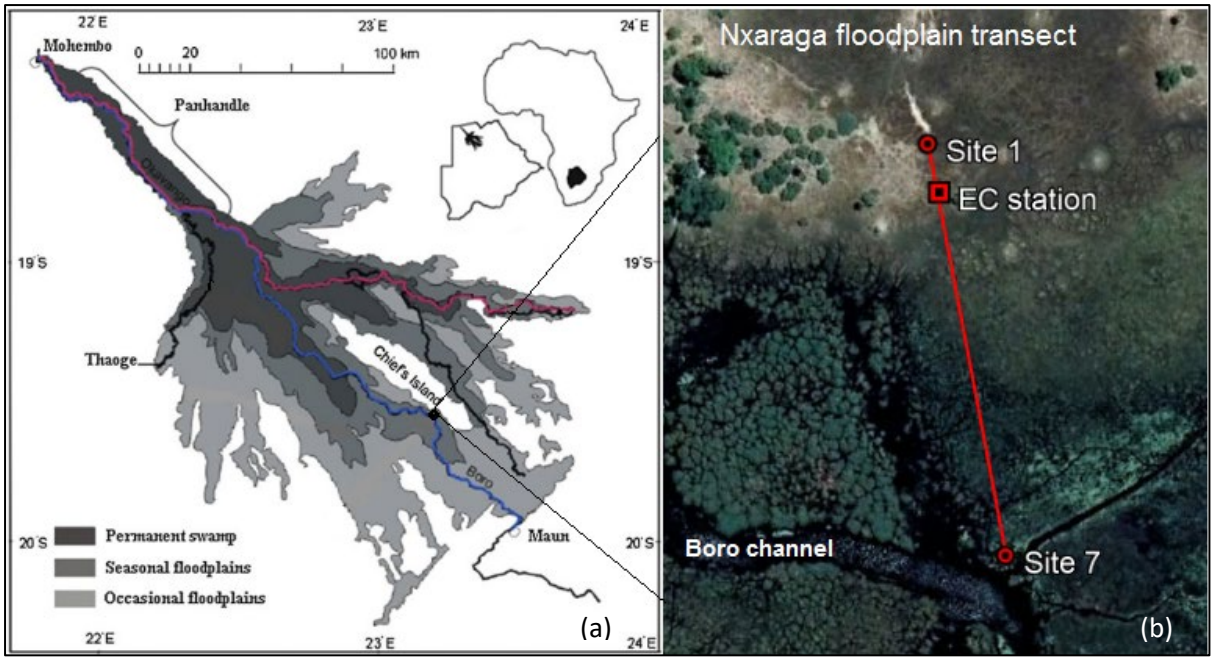

Figure 1. Map of the Okavango Delta (a) showing the study location and study transect across the seasonal floodplain at Nxaraga (b). The transect was oriented along the predominant southerly wind direction at Nxaraga.

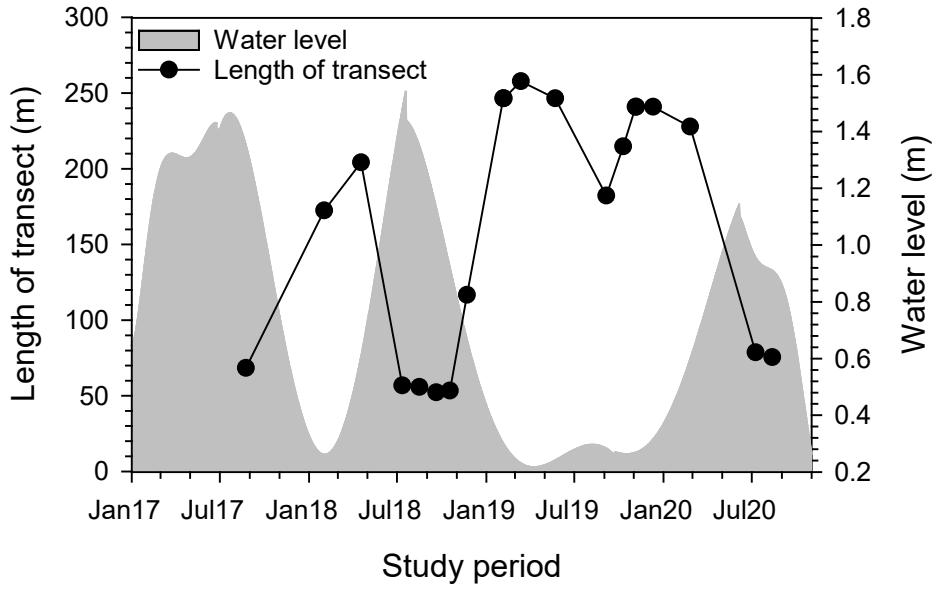

Figure 2. Variations in the length of the sampling transect due to seasonal flooding illustrated by water level in the bordering Boro channel at Nxaraga (Figure 1b). Transects spanned Site 1 (at 0 m transect length) to the flood water front or edge of Boro channel (dark circles) as the water expanded or receded in the floodplain. Longest (e.g., >200 m) and shortest (~50 m) transects were, respectively, sampled during lowstand and highstand flood extents in the seasonal floodplain. See Figure 3 for a schematic diagram of the floodplain cross-section at highstand and lowstand flood extents.

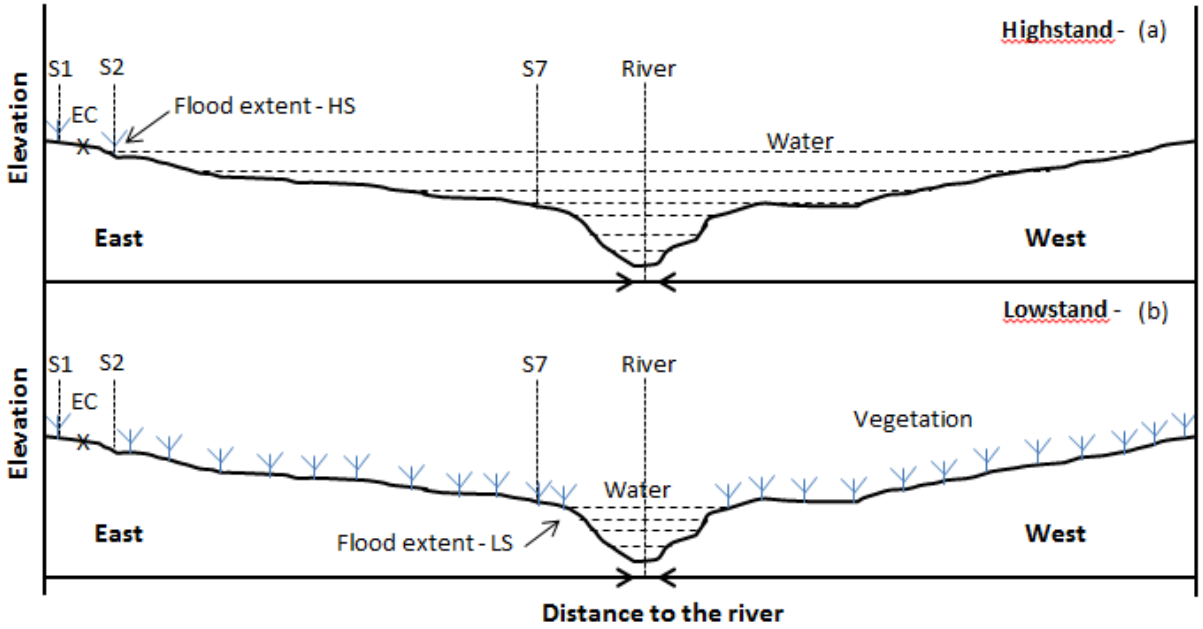

632

633 Figure 3. Schematic diagram of the highstand (a) and lowstand (b) flood extents in the seasonal
634 floodplain at Nxaraga. The flood extent during a particular sampling campaign determined the
635 length of that campaign's sample transect across the seasonal floodplain. The sample transect
636 was longest at lowstand and shortest at highstand flood extents. For plant species and
637 distribution across the seasonal floodplain see [27].

638

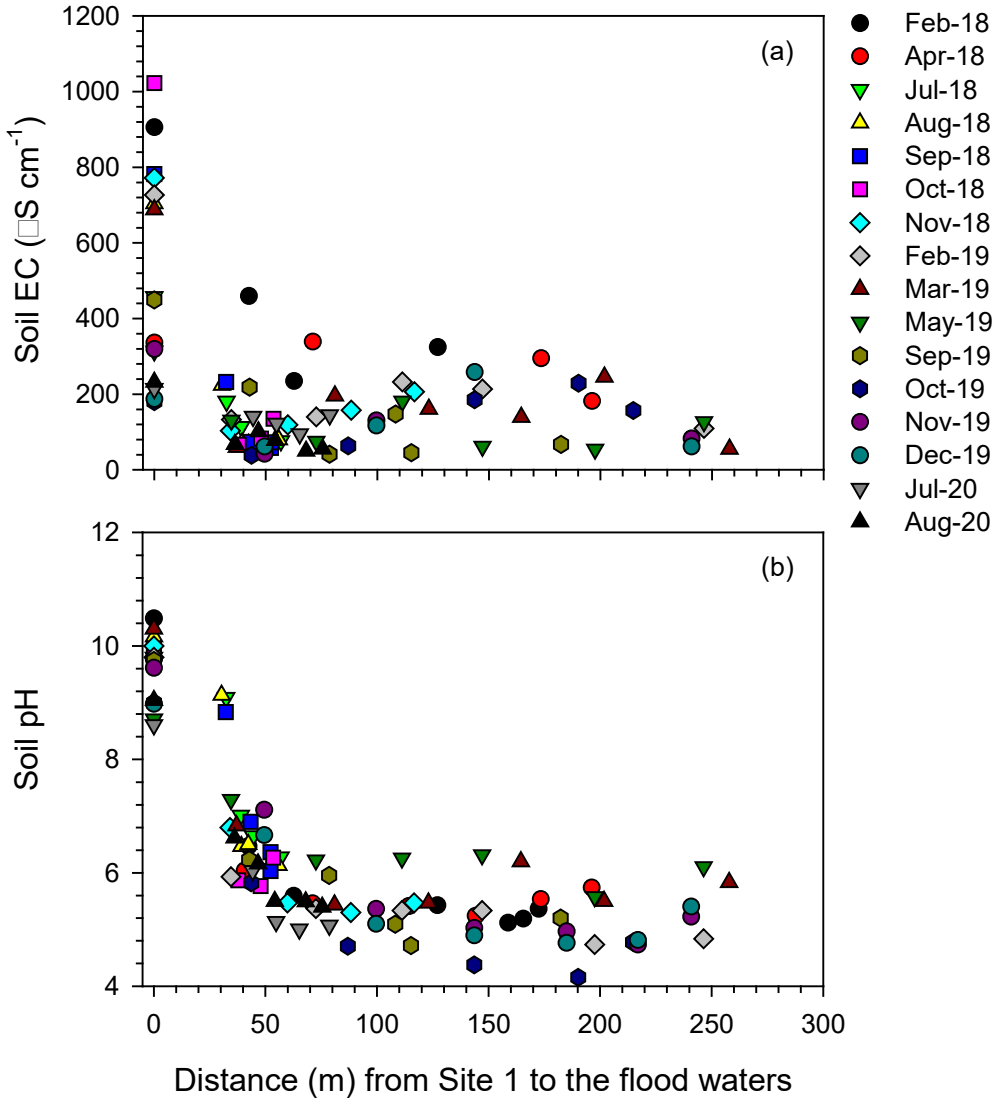

Figure 4. Variations of soil EC (a) and soil pH (b) along a transect (Site 1-7) across a seasonal floodplain at Nxaraga. The data are the means of 3 replicates per sampling site for soil pH and soil EC obtained during the monthly 2-day sampling campaigns. The legend will be the same for the rest of the figures unless legend is provided for that figure.

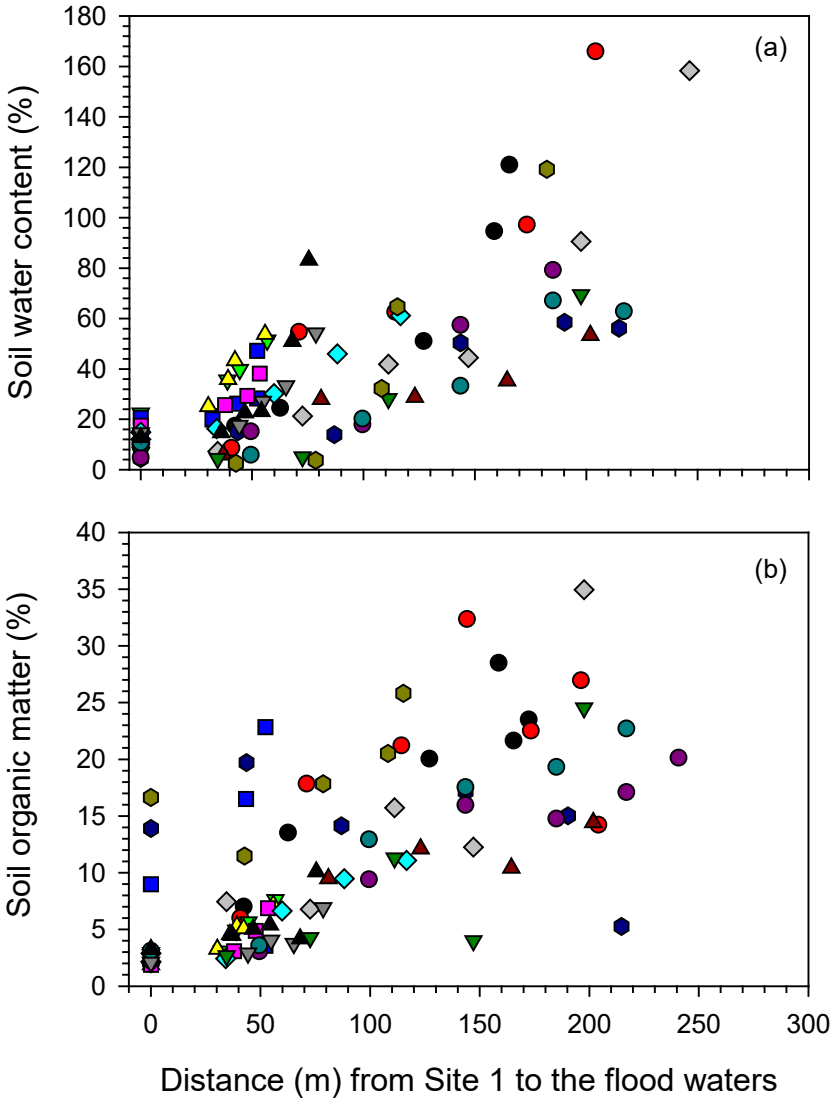

650

651 Figure 5. Variations of soil water content (a) and soil organic matter (b) along a transect (Site
652 1-7) across a seasonal floodplain at Nxaraga. The data are the means of 3 replicates per
653 sampling site for SWC and SOM obtained during the monthly 2-day sampling campaigns. See
654 Figure 3 for legend.

655

656

657

658

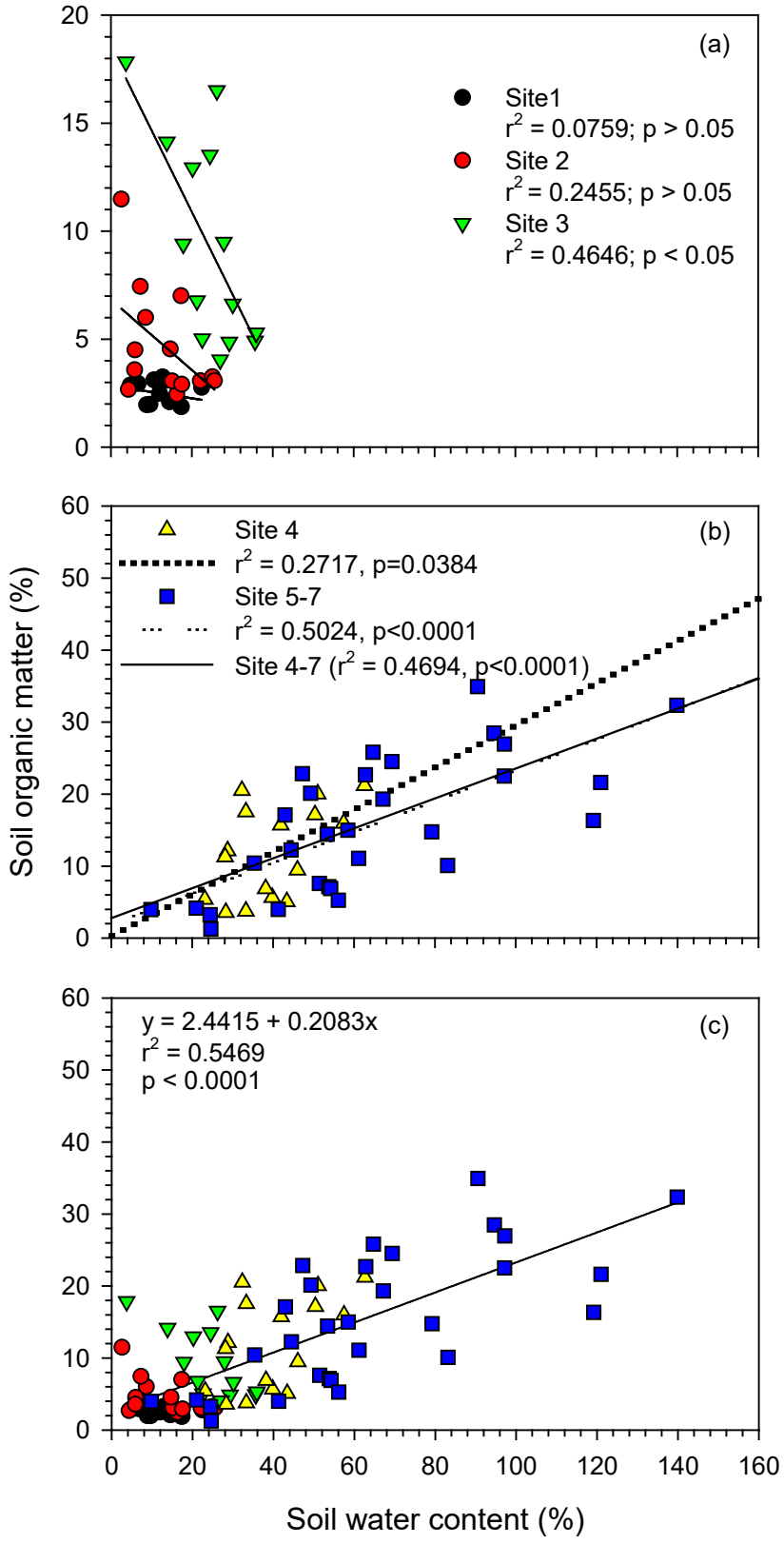

659

660 Figure 6. Relationship between soil water content (%) and soil organic matter (%) at sites 1-3
661 (a), sites 4-7 (b), and at all sites along the study transect (c) across a seasonal floodplain at

Nxaraga. The data are the means of 3 replicates per sampling site for SWC and SOM obtained during the monthly 2-day sampling campaigns. The SWC-SOM relationship was assessed at site level in (a) and (b) because of the drought condition the seasonal floodplain experienced during the study period which might have affected the littoral sites more than the wetter sites near the Boro channel.

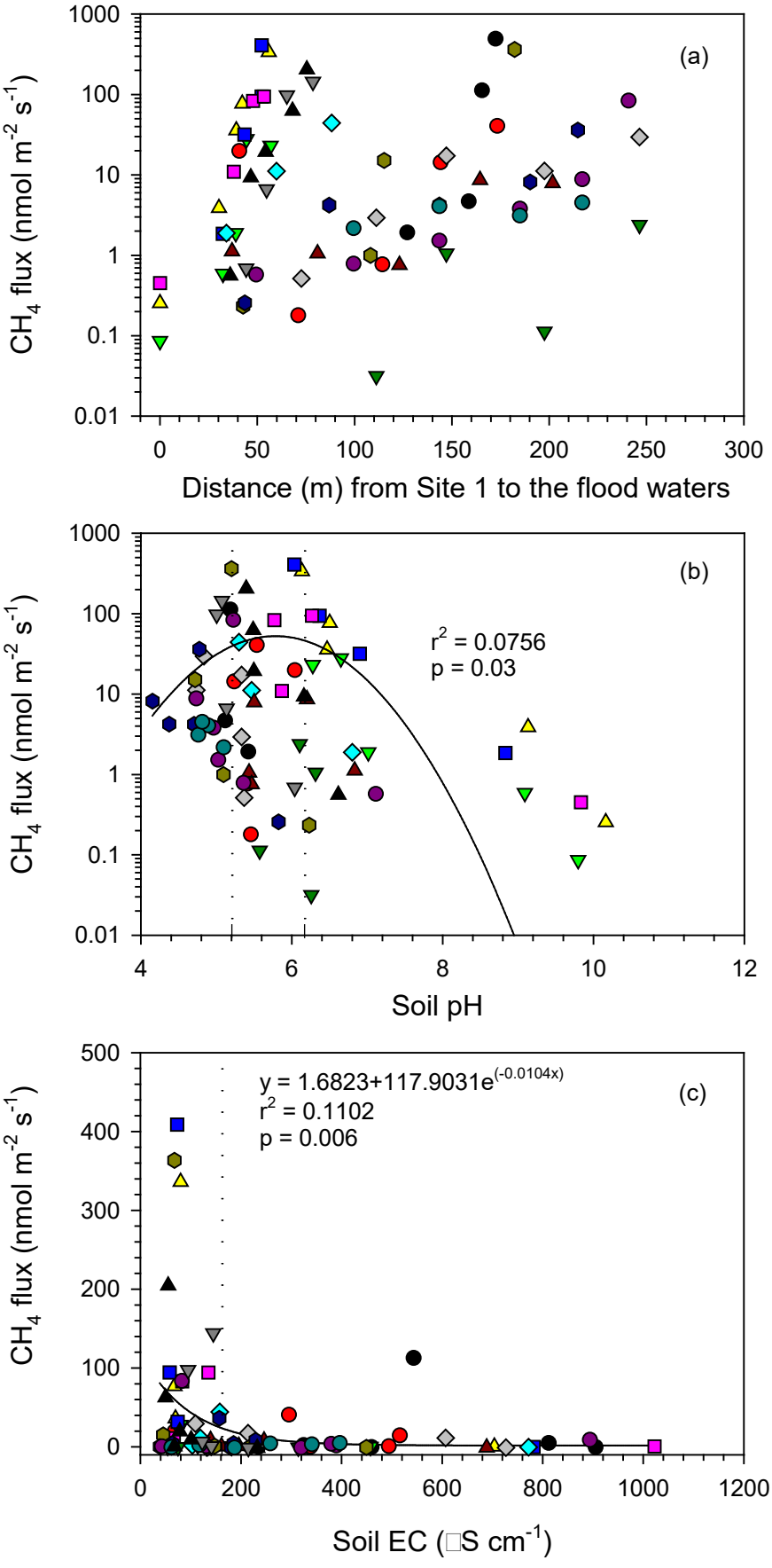
(a)
CH4 flux (nmol m-2 s-1)
Distance (m) from Site 1 to the flood waters
(b)
r2 = 0.0756
p = 0.03
Soil pH
(c)
y = 1.6823+117.9031e(-0.0104x)
r2 = 0.1102
p = 0.006
Soil EC (□S cm-1)

667

Figure 7. Variation of mean monthly CH_4 fluxes with distance along the study transect (a) and its relationship with soil pH (b) and soil EC (c) in a seasonal floodplain at Nxaraga. The data are the means of 3 replicates per sampling site for soil pH, soil EC and soil CH_4 fluxes obtained during the monthly 2-day sampling campaigns. The dashed lines in (b) & (c) indicate the optimum range of soil pH (pH 5.2-6.2) and soil EC (< 160 µS cm^{-1}) for soil CH_4 flux in the seasonal floodplain at Nxaraga. See Figure 3 for legend.

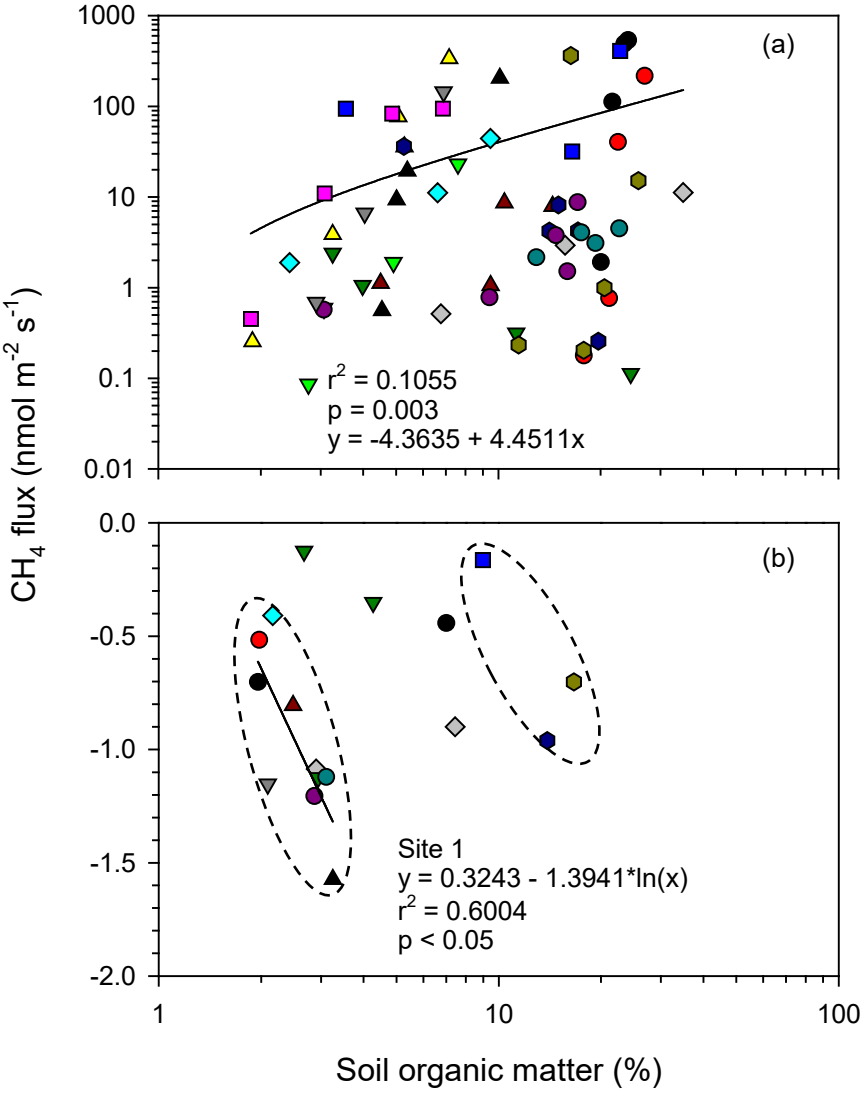

Figure 8. Relationship between soil organic matter (%) and CH_4 emissions (a), and CH_4 oxidation (b) in a seasonal floodplain at Nxaraga. The data are the means of 3 replicates per sampling site for SOM and soil CH_4 fluxes obtained during the monthly 2-day sampling campaigns. The mean monthly CH_4 oxidation fluxes in (b) were measured at Site 1 (in circles) and at Site 2 (outside the circles). See Figure 3 for legend.

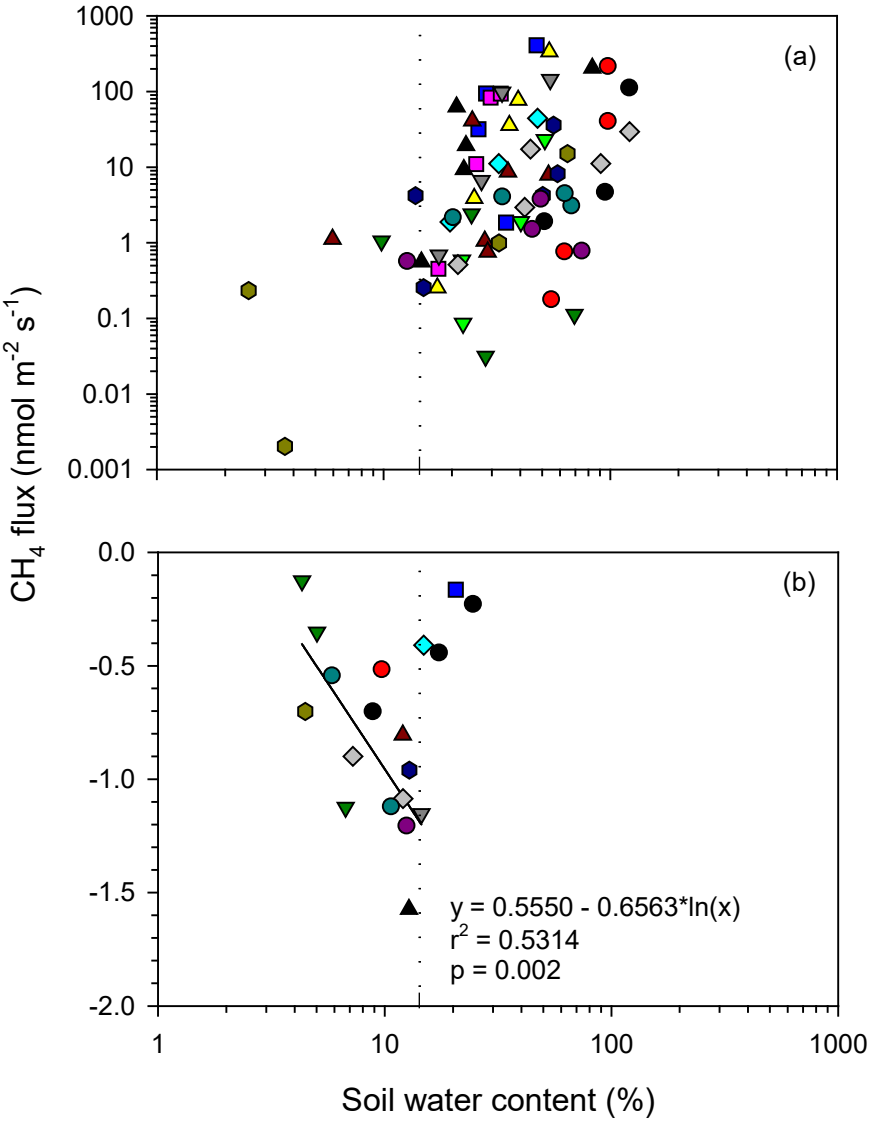

682

683 Figure 9. Relationship between soil water content and soil CH_4 emissions (a) and CH_4 oxidation
684 (b) in a seasonal floodplain at Nxaraga. The data are the means of 3 replicates per sampling
685 site for SWC and soil CH_4 fluxes obtained during the monthly 2-day sampling campaigns. The
686 dashed line indicates SWC at which soil CH_4 oxidation (b) is optimum at 15% SWC. See Figure
687 3 for legend.

688

689

690

691

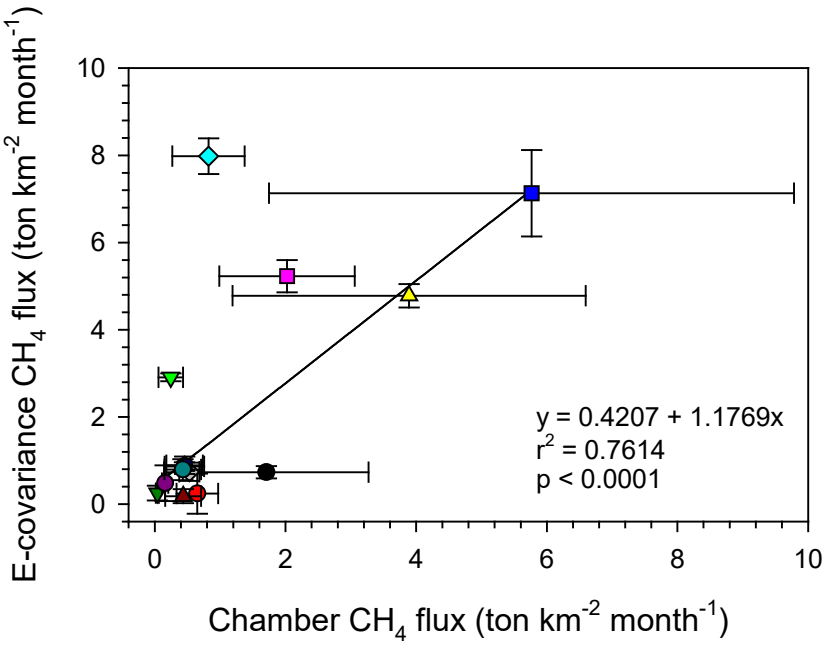

Figure 10. Correlation between Chamber-CH_4 fluxes and EC-CH_4 fluxes measured with closed dynamic chamber and eddy-covariance techniques respectively at Nxaraga seasonal floodplain in 2018 and 2019. The chamber flux data are the means of chamber site 2-7 obtained for each monthly day of sampling. The eddy-covariance flux is the conditional monthly mean of all available data points in the [130°, 270°] wind sector for which 90% of the measured flux originated within 200 m from the instrument mast. This condition was imposed to ensure that the flux footprint of the eddy-covariance system was limited to the portion of the floodplain where chamber sampling occurred. CH_4 flux for Nov-18 (see legend in Figure 4) was excluded for curve fitting.